Supporting Information

Precisely tunable thickness of graphitic carbon nitride nanosheets for visible-light-driven photocatalytic hydrogen evolution

Yuanzhi Hong[a], Changsheng Li[a], Di Li[b], Zhenyuan Fang[c], Bifu Luo[c], Xu Yan[c], Hongqiang Shen[c], Baodong Mao[c], Weidong Shi[c]*

[a]*School of Materials Science and Engineering, Jiangsu University, Zhenjiang, 212013, P. R. China*

[b]*Institute for Energy Research, Jiangsu University, Zhenjiang, 212013, P. R. China*

[c]*School of Chemistry and Chemical Engineering, Jiangsu University, Zhenjiang, 212013, P. R. China*

E-mail: swd1978@ujs.edu.cn (W. Shi)

Figure and Table Captions

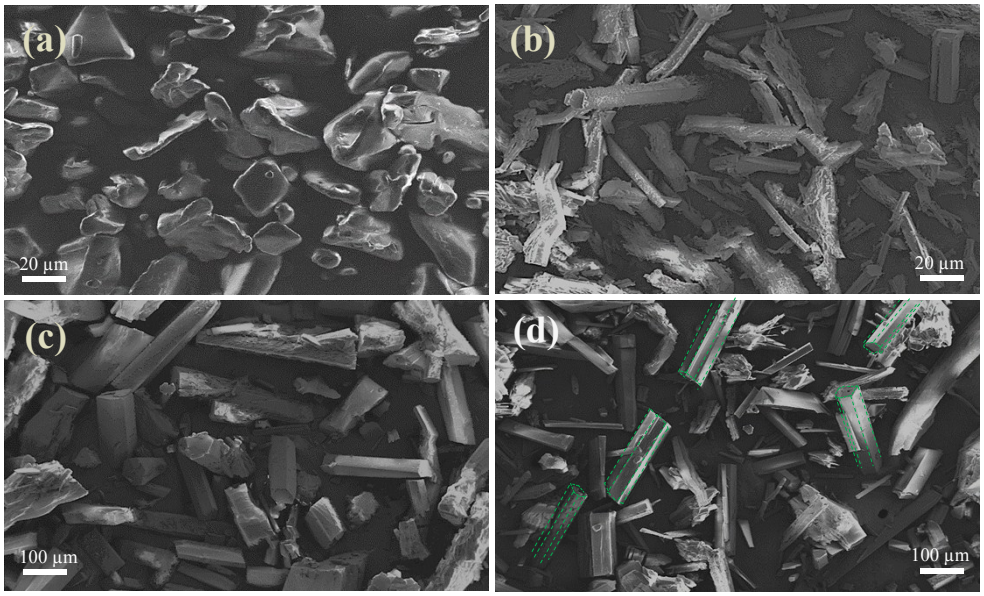

Figure S1 SEM images of the different precursors: (a) pristine melamine; (b) MSA-0.5; (c) MSA-1.5; (d) MSA-2.5.

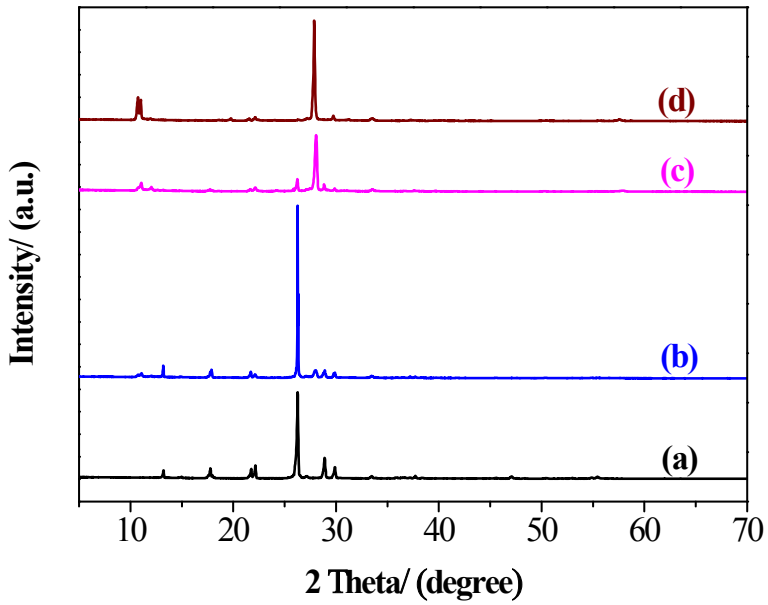

Figure S2 XRD patterns of the different precursors: (a) pristine melamine; (b) MSA-0.5; (c) MSA-1.5; (d) MSA-2.5.

SEM image (Figure S1) reveals that pristine melamine exhibits the stone-like particles with an average diameter of 25 μm. The as-prepared MSA-0.5 shows the non-standard stick structure with a length of around 50 μm, whereas the MSA-1.5 shows the irregular cube structure with a length of 150-200 μm. When further increased the HCl content, the MSA-2.5 depicts the hexagonal rod-like architecture with smooth surface in a length of around 200 μm. XRD spectra (Figure S2) illustrates that the crystal structure of the as-obtained MSA precursors were obviously changed with increasing the HCl amount. The results indicate that the morphology and crystal structure of the as-made melamine-based supramolecular aggregates are strongly influenced by the HCl concentration.

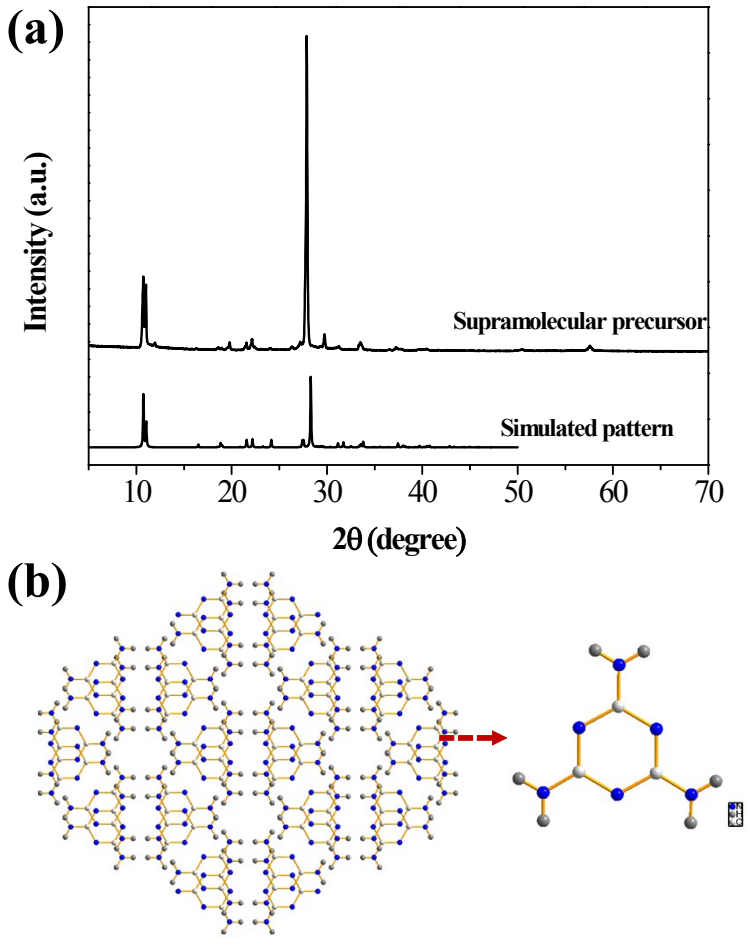

Figure S3 (a) XRD patterns of the MSA-2.5 and the simulated patterns; (b) single crystalline structure of as-synthesized MSA-2.5 precursor. Packing analysis using the single crystalline precursor shows that melamine molecules are held together by the hydrogen bonds to forming the melamine-based supramolecular structure. There is no HCl found in the precursor structure, suggesting the HCl plays an induced role on the synthesis of the melamine supramolecular.

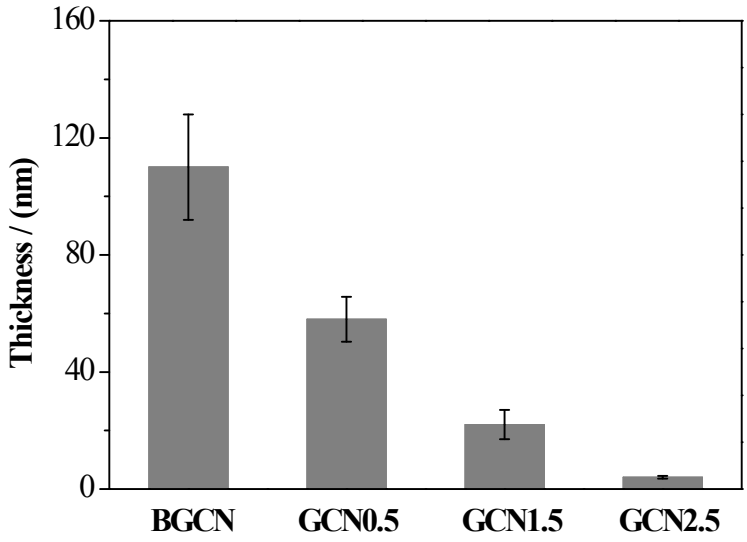

Figure S4 The average thickness of as-prepared BGCN, GCN0.5, GCN1.5 and GCN2.5 samples with error bars.

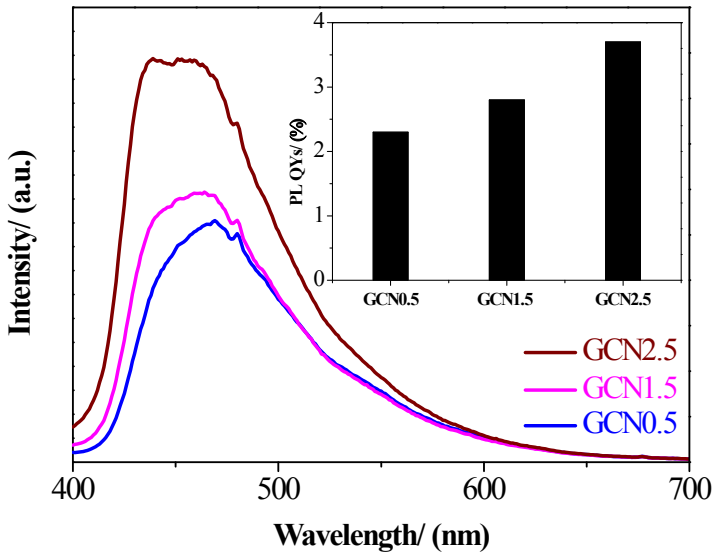

Figure S5 PL emission spectra of as-prepared samples. The inset is their PL QYs.

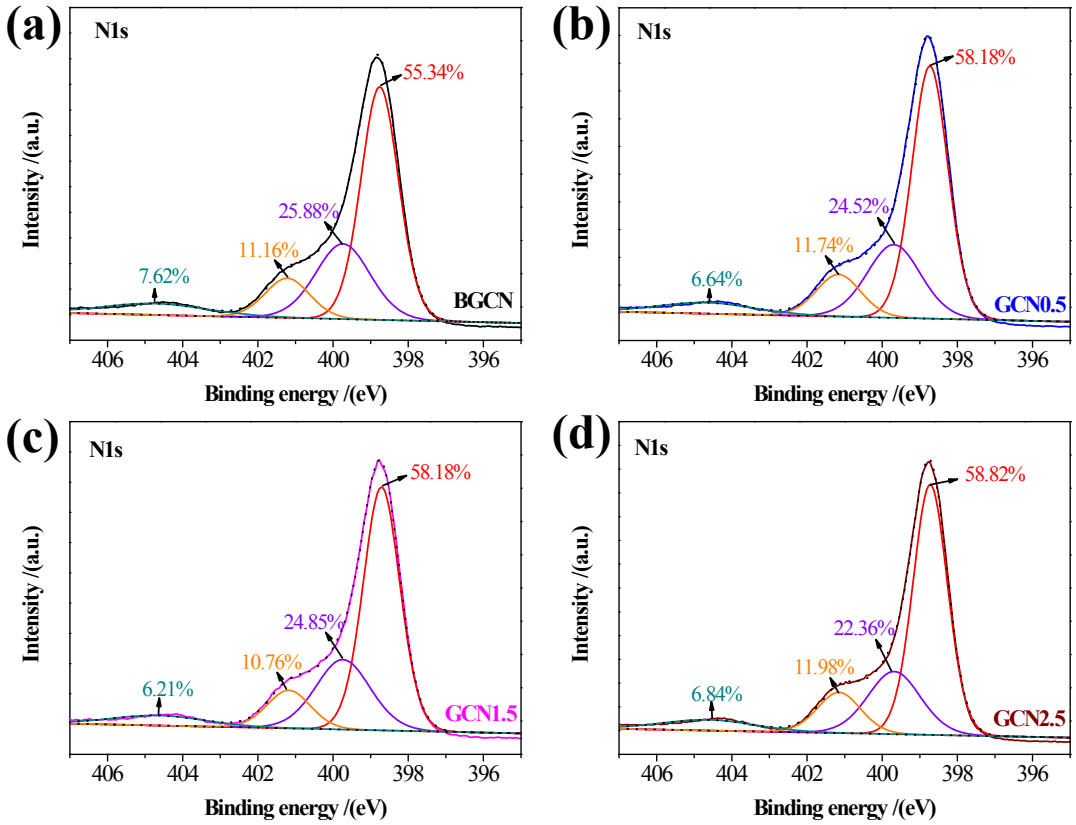

Figure S6 The high-resolution N1s XPS spectra of as-prepared samples: (a) BGCN, (b) GCN0.5, (c) GCN1.5, and (d) GCN2.5.

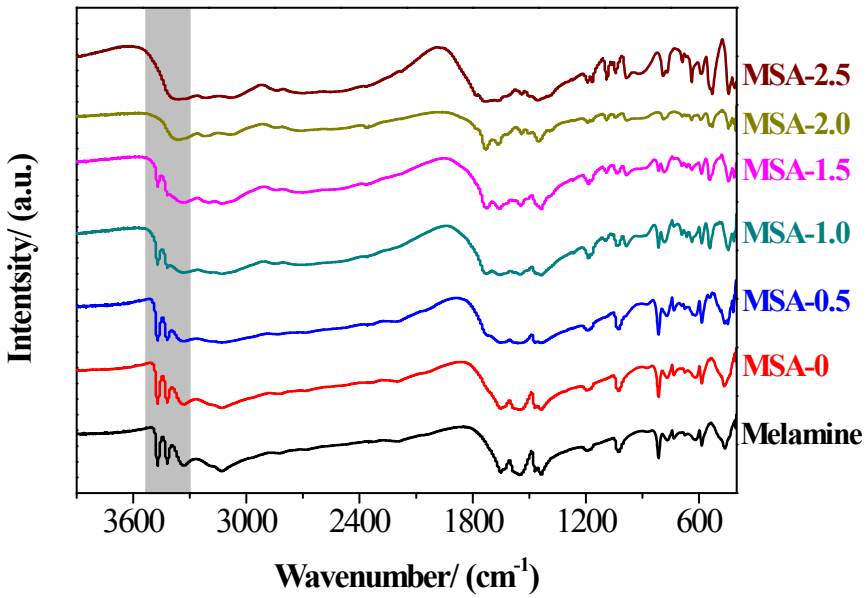

Figure S7 The FT-IR spectra of as-formed MSA precursors.

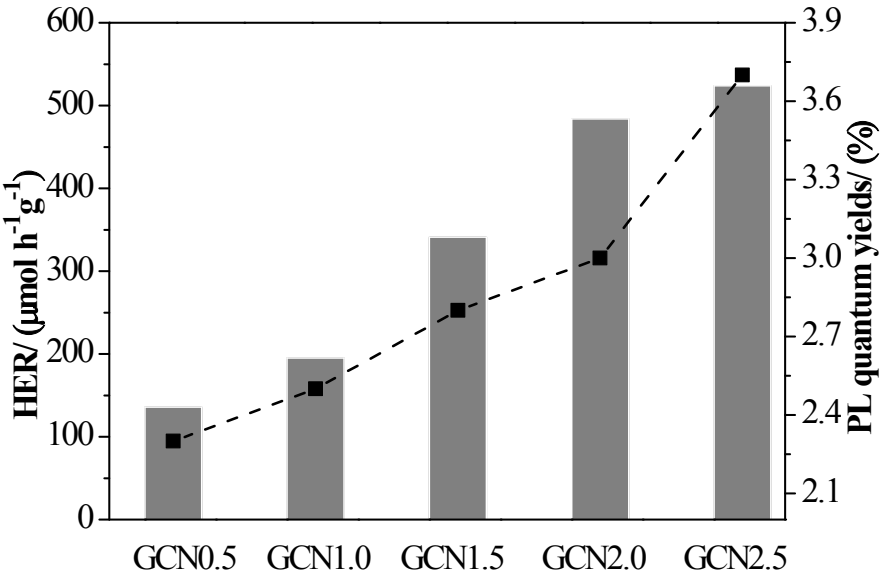

Figure S8 The PL QYs vs. HER of as-prepared GCN nanosheets.

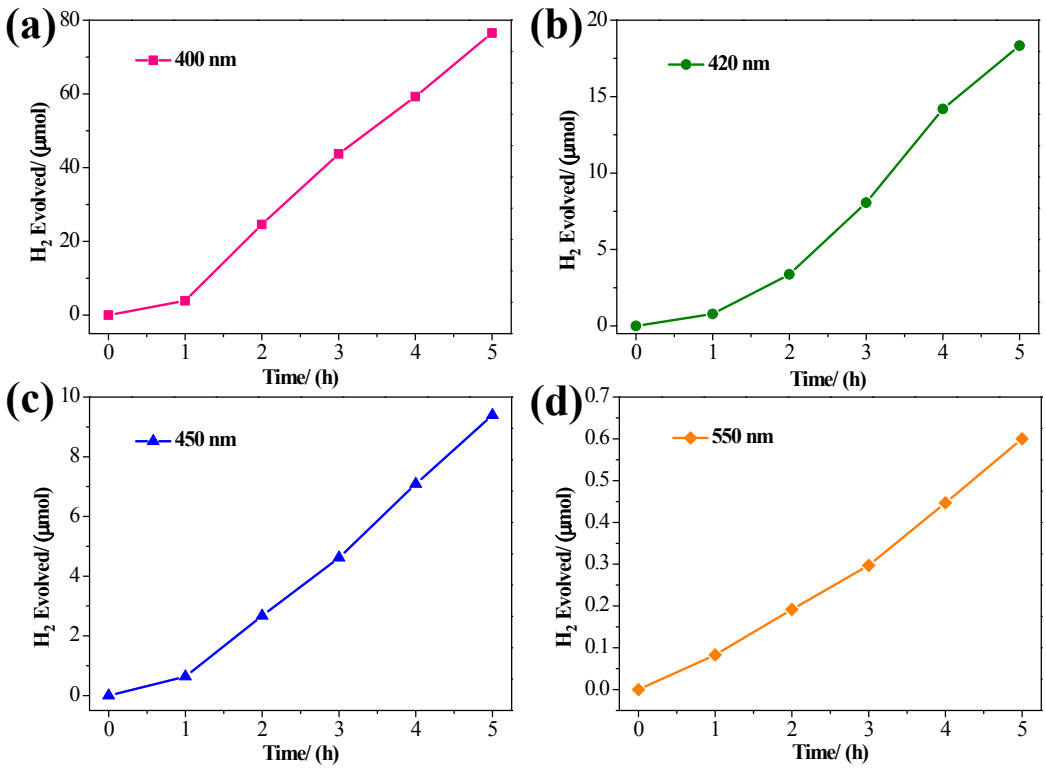

Figure S9 Time courses of photocatalytic hydrogen evolution over the GCN2.5 nanosheets under different wavelength numbers: (a) 400 nm, (b) 420 nm, (c) 450 nm, and (d) 550 nm.

The apparent quantum efficiency (AQE) of GCN2.5 nanosheets for H_2 evolution had been measured by the following equation:

$$AQE = \frac{2 \times the\ number\ of\ evolved\ H_2 molecules}{the\ number\ of\ incident\ photos}$$

where the average intensity of irradiation at λ = 400 nm was determined to be 72.0 $mW.cm^{-2}$ by a CEL-NP2000 optical power densitometer, and the irradiation area was 24.6 cm^2. The amount of H_2 molecules of GCN2.5 nanosheets generated in 5 h was 76.5 μmol. Thus, the apparent quantum efficiency of the GCN2.5 photocatalyst was determined as 0.144% at 400 nm.

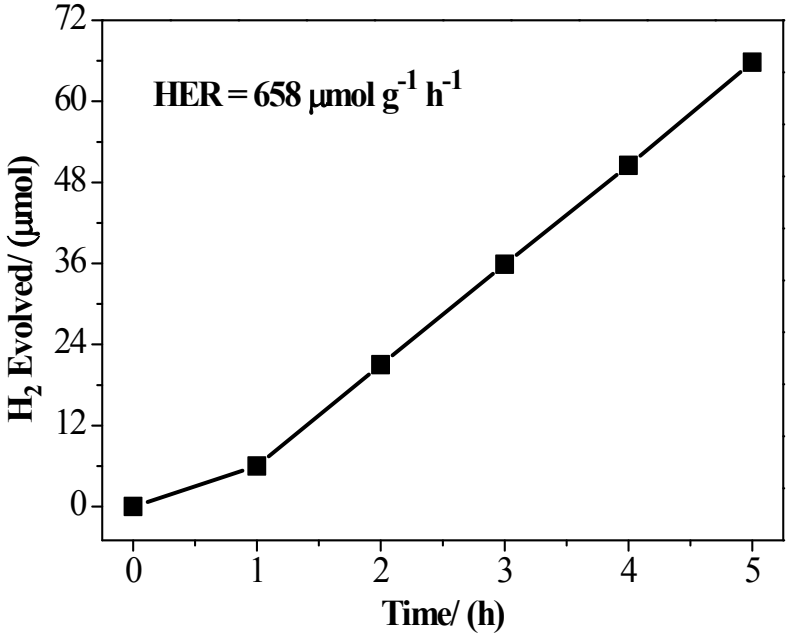

Figure S10 Time courses of photocatalytic hydrogen evolution over the ultrathin GCN nanosheets prepared from the thermal oxidation etching.

Table S1 Summary of the previously reported GCN nanosheets photocatalysts for HER rate, surface area, and increased HER fold than BGCN.

Samples	HER rate μmol h^{-1} g^{-1}	Surface area m^2 g^{-1}	Increased HER fold than BGCN	Ref.
GCN nanosheets	650	306	3	1
	1860	384	9.3	2
	230	205.8	2.6	3
	420	80	3.1	4
	1171	42	6	5
	503.8	44.4	6	6
	552.9	99.7	6.8	7
	524	**170**	**9**	This work

References

1 P. Niu, L. Zhang, G. Liu and H. M. Cheng, *Adv. Funct. Mater.*, 2012, **22**, 4763-4770.

2 S. Yang, Y. Gong, J. Zhang, L. Zhan, L. Ma, Z. Fang, R. Vajtai, X. Wang and P. M. Ajayan, *Adv. Mater.*, 2013, **25**, 2452-2457.

3 J. Xu, L. Zhang, R. Shi and Y. Zhu, *J. Mater. Chem. A*, 2013, **1**, 14766-14772.

4 J. Tong, L. Zhang, F. Li, M. Li and S. Cao, *Phys. Chem. Chem. Phys.*, 2015, **17**, 23532-23537.

5 W. Xing, G. Chen, C. Li, J. Sun, Z. Han, Y. Zhou, Y. Hu and Q. Meng, *ChemCatChem*, 2016, **8**, 2838-2845.

6 Y. Hong, C. Li, Z. Fang, B. Luo and W. Shi, *Carbon*, 2017, **121**, 463-471.

7 D. Zhao, J. Chen, C.L. Dong, W. Zhou, Y.C. Huang, S.S. Mao, L. Guo and S. Shen, *J. Catal.*, 2017, **352**, 491-497.